JET–P(98)53

J G Cordey et al

Plasma Confinement in JET H-mode Plasmas with H, D, D-T and T Isotopes

JET–P(98)53

Plasma Confinement in JET H-mode Plasmas with H, D, D-T and T Isotopes

J G Cordey, B Balet, D V Bartlett, R Budny[1], J P Christiansen, G D Conway, L-G Eriksson, G Fishpool, C W Gowers, J C M de Haas[2], P J Harbour, L D Horton, A C Howman, J G Jacquinot, W O K Kerner, C G Lowry, R D Monk, P Nielsen, F G Rimini, G R Saibene, R Sartori, B Schunke, A C C Sips, R J Smith, M F Stamp, D F H Start, K Thomsen, B J D Tubbing.

JET Joint Undertaking, Abingdon, Oxfordshire, OX14 3EA,
[1]PPPL Princeton University, Princeton, NJ, USA.
[2]Netherlands Foundation for Research in Astronomy, Dwingeloo, The Netherlands.

Preprint of a Paper to be submitted for publication in Nuclear Fusion

December 1998

ABSTRACT

The scaling of the energy confinement in H-mode plasmas with different hydrogenic isotopes (H, D, D-T and T) is investigated in JET. For ELM-free H-modes the thermal energy confinement time τ_{th} is found to decrease weakly with the isotope mass ($\tau_{th} \sim M^{-0.25 \pm 0.22}$) whilst in ELMy H-modes the energy confinement time shows practically no mass dependence ($\tau_{th} \sim M^{0.03 \pm 0.1}$). Detailed local transport analysis of the ELMy H-mode plasmas reveals that the confinement in the edge region increases strongly with the isotope mass whereas the confinement in the core region decreases with mass ($\tau_{thcore} \propto M^{-0.16}$) in approximate agreement with theoretical models of the gyro-Bohm type ($\tau_{gB} \sim M^{-0.2}$).

1. INTRODUCTION

The scaling of the thermal energy confinement τ_{th} with the isotope mass M has been studied extensively on many devices using mainly hydrogen and deuterium isotopes [1-4]. More recently studies were completed in TFTR [5] with mixtures of deuterium and tritium in a variety of pulse types. For all pulse types the confinement increased with isotope mass $\tau_{th} \propto M^{\alpha}$ with α ranging from $0 \rightarrow 0.85$. A positive value for α is in conflict with simple theoretical expectations, from which one would expect a small negative value for gyro-Bohm turbulence ($\alpha = -0.2$) and $\alpha = 0$ for long wavelength turbulence of the Bohm type. Various explanations have been put forward by the theoretical community to explain this discrepancey, such as the effect of the different isotopes on the shear flow and the resultant modification of the ion-temperature gradient driven turbulence.

Previous JET investigations [4] of the scaling of confinement with ion mass were in L-mode plasmas and H, D and He^3 isotopes were used. The hydrogen-deuterium comparison gave a weak scaling with mass $\tau_{th} \propto M^{0.2}$ and the H_e^3 and D comparison gave no change in τ_{th} with mass at all. Likewise there was no mass scaling of τ_{th} in ohmic plasmas, this at least seems to be a common result in all the devices.

During 1997 a campaign of D-T experiments was carried out on JET mainly in H-mode plasmas and this was then followed up by a short hydrogen campaign. An overview of the results from the D-T campaign has been presented elsewhere [6]; in this paper we concentrate entirely on the scaling of the confinement and transport with the isotope mass. The main study was in the ELMy H-mode regime, the perceived operational mode for ITER, the next step device, although data on the mass scaling of the ohmic, L-mode and ELM-free regions have been obtained. In all regimes we find that the global confinement scaling is only weakly dependent on the mass. A key result is that in the ELMy H-mode we find that the plasma core has a mass scaling which is in line with gyro-Bohm scaling i.e. τ_{th} decreasing with mass whilst in the edge region the scaling of τ_{th} is strongly positive with mass, in particular the edge pedestal energy is almost proportional to the mass. The combination of these two opposing mass scalings gives rise to the approximate mass independence of the total scaling.

The paper is structured as follows. In section II we give a brief summary of the mass dependence of some of the present H-mode scaling expressions obtained from the ITER database [7-8]. Section II also lists the expected mass scaling of a few basic theoretical models for the plasma transport. Then in section III we present the main experimental results on the global confinement scaling of a selected set of JET discharges. In section IV the scaling of the edge and core regions are examined and in section V the local transport analysis from the TRANSP code is presented. This analysis is found to confirm the different mass scaling of the core and edge regions. The main conclusions of the paper are then listed in section VI.

II. EMPIRICAL AND THEORETICAL CONFINEMENT SCALINGS OF H-MODE PLASMAS

The ITER multi-machine database group has recently published a log linear scaling [7] for the thermal energy confinement time τ_{th} of ELMy H-modes, in terms of the engineering parameters this has the form:

$$\tau_{ITERH-EPS97(y)} = 0.029\, I^{0.90}\, B^{0.20}\, P^{-0.66}\, n^{0.40}\, R^{2.03}\, \varepsilon^{0.19}\, \kappa^{0.92}\, M^{0.2} \qquad (1)$$

where the variables and units are τ_{th}(s) energy confinement time, I (MA) current, B(T) toroidal field, P(MW) loss power, n ($\times 10^{19}$ m $^{-3}$) density, R(m) major radius, ε inverse aspect ratio a/R, κ elongation and M the effective mass.

A new expression was also derived in reference (7) for the ELM-free scaling however this was almost identical to the ITERH93-P [8] ELM-free scaling. Hence we shall compare the ITERH93-P expression with the data, this has the form

$$\tau_{ITERH-93P} = 0.036\, I^{1.06}\, B^{0.32}\, P^{-0.67}\, n^{0.17}\, R^{1.79}\, \varepsilon^{-0.11}\, \kappa^{0.66}\, M^{0.41} \qquad (2)$$

where the variables and units are the same as for Eq. (1)

Both of these forms satisfy the high β Kadomtsev constraint in terms of the dimensionless physics parameters (ρ^* normalised Larmor radius, ν^* collisionality, β beta), they have the form:

$$\frac{B\tau_{ITERH-EPS97(y)}}{M} \propto \rho^{*-2.88}\, \beta^{-0.68}\, \nu^{*-0.09}\, M^{1.03} \qquad \text{ELMy} \qquad (3)$$

$$\frac{B\tau_{ITERH-93P}}{M} \propto \rho^{*-2.81}\, \beta^{-1.22}\, \nu^{*-0.30}\, M^{1.61} \qquad \text{ELM-free} \qquad (4)$$

Both these scalings have a positive mass dependence, with the ELM-free scaling being stronger than the ELMy. The mass dependence arises through comparisons of hydrogen and deuterium data mainly from the smaller devices in the database. A further scaling for ELMy H-modes with an even weaker mass dependence $M^{0.11}$, has also been derived in reference [7], by equal weighting of the machines in the database.

Most theoretical models, but not all, assume that the turbulence which produces the transport has a scale-length of the order of the ion Larmor radius ρ_i with a decorrelation time of the ion diamagnetic drift time $(\omega^*)^{-1}$. The resulting thermal diffusivity would then scale as follows:

$$\chi \sim \omega^* \rho_i^2 \sim \kappa_\theta \rho_i \frac{V_{th}}{L_n} \rho_i^2 \sim \frac{T}{B} \frac{T^{1/2} M^{1/2}}{B L_n} \tag{5}$$

Here it has been assumed that the dominant poloidal wavenumber $\kappa_\theta \sim 1/\rho_{i.}$

Eq. (5) shows that χ should scale as $M^{1/2}$ with a resulting scaling for τ_{th} given by $\tau_{th} \sim \frac{Ba^2}{T} \frac{BL_n}{T^{1/2} M^{1/2}}$. Converting this expression to the conventional form as a function of the power P and density n etc. it becomes,

$$\tau_{th} \propto B^{4/5}\, a^3\, n^{3/5}\, P^{-3/5}\, M^{-1/5} \tag{6}$$

where we have assumed $L_n \sim a$, the minor radius.

Hence in this form τ_{th} should decrease weakly with mass M. One can derive similar scalings for long wavelength turbulent (Bohm) transport and stochastic transport, here the mass dependence is found to be M^0 for Bohm and $M^{1/5}$ for stochastic transport. Although the precise value of the index in the stochastic transport will depend on the β dependence of the loss mechanism it will nevertheless always be positive. The fact that all of the above scalings have a weak mass dependence, implies that physical mechanisms other than conventional turbulent transport (such as atomic physics processes) must be responsible for the strong mass dependent scalings reported in some of the devices.

III. GLOBAL CONFINEMENT SCALING

The set of discharges that have been used in the analysis have the same geometry and the set includes H, D, D-T, T discharges. The heating of the discharges was by Ion Cyclotron Resonant Heating and neutral beam injection where the same species was injected as the background plasma. Care was also taken fully to condition the walls with the same plasma specie as the main plasma. Discharges were at a fixed $q_{\psi 95}$ = 3.4 apart from one high fusion yield D-T pulse at a q_{95}=2.7. The remainder of the geometrical and plasma parameters for the set of pulses are listed in Table I.

Table I

Parameter	**Value**
R (M)	2.88
a (M)	0.93
κ/δ	1.7/0.2-03
B (T)	1-4
I (MA)	1-4.5
P (MW)	4-25
$\langle n \rangle$ (10^{19} m^{-3})	1.8-8
q_{95}	2.7-3.4

The stored energy is measured by two different techniques, a) by the diamagnetic loop and b) a full kinetic analysis. To evaluate the thermal stored energy from the diamagnetic measurement, the fast ion contribution is calculated numerically using the PENCIL Fokker Planck code, which has been benchmarked against the TRANSP code. In the kinetic analysis the electron temperature and density are obtained from Thomson scattering measurements (Lidar [9]) and the ion temperature and Zeff from the charge exchange recombination diagnostic [10]. The two techniques are found to be in close agreement for the complete set of pulses. For the remainder of this section the first technique is used. The isotope concentration was measured spectroscopically through the ratio of the $T\alpha/D\alpha$ or $H\alpha/D\alpha$ lines at close to the outer strike point and used to estimate an effective mass, M, defined as $M = (n_H + 2\,n_D + 3n_T)/(n_H + n_D + n_T)$.

a) ELM-free scaling

Significant ELM-free phases were seen in the D, D-T and T plasmas, however in the hydrogen plasmas no clear ELM free phases were observed. The longest ELM-free phases are observed in the Hot-ion H-mode regime described in [11].

In Fig. (1) the thermal energy confinement time is shown versus the ELM-free scaling ITERH-93P. From the figure it can be seen that the confinement in the pure tritium data is systematically below that of the deuterium which suggests that the strong mass dependence of ITERH-93P i.e. $M^{0.41}$ is probably incorrect. Refitting the data by using the same form as equation (2) but allowing the mass dependence and the constant to be varied, results in a better fit

$$\tau_{th} = 1.1\ \tau_{ITERH\text{-}93P}\,(M/2)^{-0.65} \qquad (7)$$

This reduces to a scaling of τ_{th} with mass which is actually negative $\tau_{th} \propto M^{-0.25 \pm 0.22}$ and in line with the expectations of gyro-Bohm scaling, Eq. (6).

Introducing this D-T data set into the full ITER multi-machine database may result in the other dependences (i.e. such as P or n) being changed and as a consequence this may result in a smaller change in the mass dependence. Nevertheless the mass dependence of the ITER93H scaling expression is too strong to describe these discharges. The effect on the predicted ITER ELM-free confinement time of the mass dependence with a negative exponent is only small, since the decrease in energy confinement time due to this mass dependence is partially offset by the increase in the constant term.

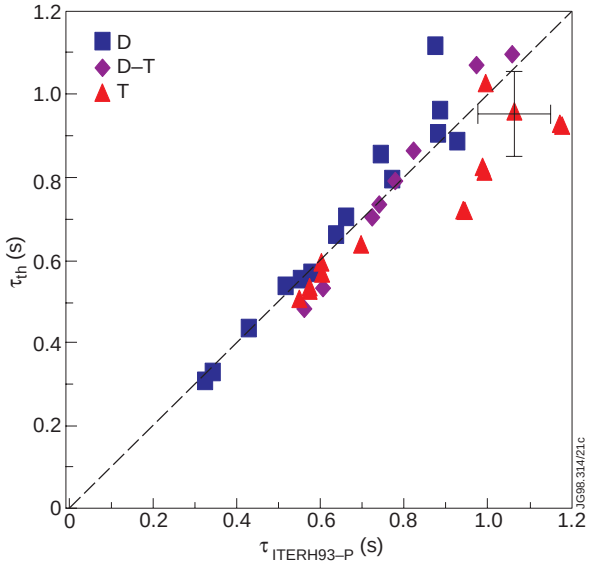

Fig. 1. Comparison of the τ_{th} for the ELM-free data versus the ITERH-93P ELM free scaling. The squares are the deuterium data, the diamonds the 50:50 D-T data and the triangles the tritium data (10:90 D-T).

b) ELMy Scaling

In Fig. 2 the ELMy thermal energy confinement time is compared with the ELMy scaling of Eq. (1) which has a fairly weak mass dependence $M^{0.2}$. The data is fairly well described by this scaling form as can be seen from Fig. 2 and repeating the same exercise as for the elm–free scaling, i.e. refitting the mass dependence we get

$$\tau_{th} = 1.02\ \tau_{ITERH\text{-}EPS97(y)}\,(M/2)^{-0.04\pm0.06} \qquad (8)$$
$$\propto M^{0.16\pm0.06}$$

This result indicates that only a small change in the mass dependence is required.

Comparing pairs of pulses with the same input power and density in pure D and T plasmas, suggests that the mass dependence may be weaker still. A good example is shown in Fig. 3 where the stored energy, electron density, Balmer α light D_α, T_α and power traces are shown for comparative 'pure' D and 'pure' T pulses. The densities are essentially identical and the energy in the tritium pulse is essentially the same as that of the deuterium pulse indicating that τ_{th} is independent of mass.

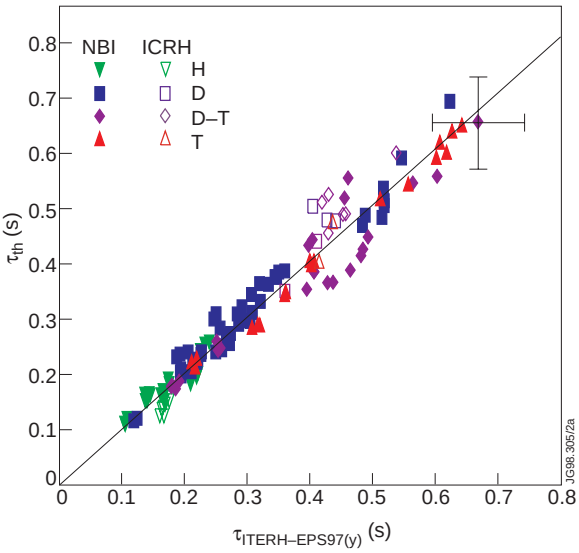

Fig. 2. Comparison of τ_{th} for the ELMy dataset with the ITERH-EPS97(y) scaling eq. (2). The solid symbols are the NBI data, the open symbols ICRH data, the symbols are t H, n D, u 50:50 D-T, and s 10:90 D-T.

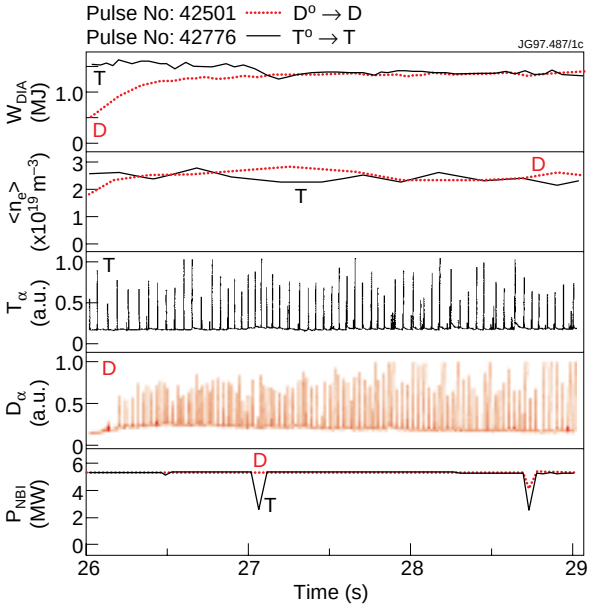

Fig. 3. Time traces for two pulses at 1MA/1T, the solid trace is for T into T and the dotted D into D. The traces are diamagnetic energy, line average density, T_α, D_α and neutral injection power.

If we constrain the dataset to pairs of pulses in D, T and H in which the density and power levels are close (powers within 5% and densities within 25%) then we find that the mass dependence of the energy confinement time is very small indeed

$$\tau_{th} \propto M^{0.03\pm0.1} \qquad (9)$$

The fit is shown in fig. 4.

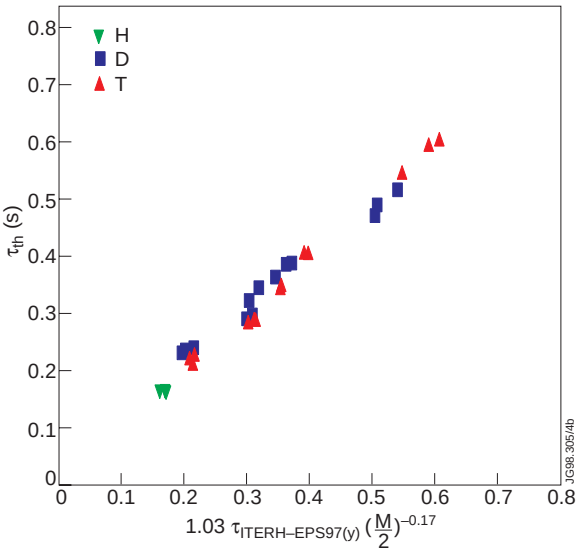

Fig. 4. Comparison of the τ_{th} for the restricted data set versus the scaling in equation (9). The data are NBI only. The symbols are `t` H, `n` D, `s` 10:90 D-T.

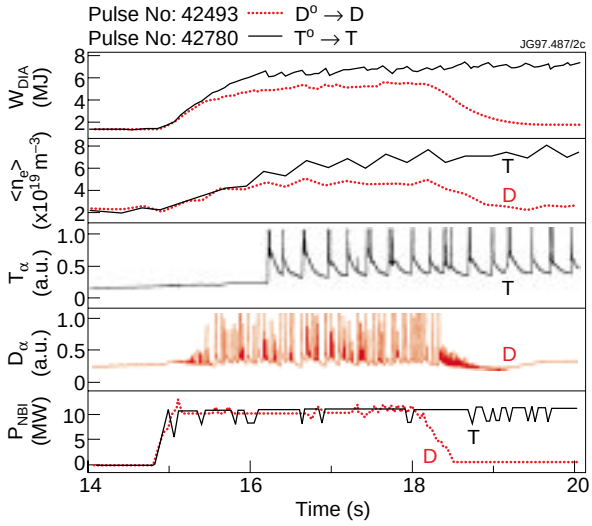

Fig. 5. Time traces for two pulses at 3MA/3T, the solid trace is for T NBI into T, and the dotted one for D into D. The traces are diamagnetic energy, line average density, T_α, D_α and neutral injection power.

A possible explanation for the lower value of the exponent of the mass dependence in this reduced dataset compared with the multi-machine scaling is due to a collinearity in the ITER database between the density and the mass dependence. In fact the JET data set itself exhibits this collinearity between density and mass very clearly at higher values of field and current. For example in Fig. 5, deuterium and tritium plasmas at 3T/3MA are compared with the same input power. The much lower density in the deuterium pulse is a consequence of the more frequent ELMs. A similar effect is seen in the hydrogen plasmas where we find that the operating density is always significant less than that of the deuterium plasmas at the same power level.

IV. SCALING OF THE EDGE PEDESTAL AND CORE CONFINEMENT

To understand the origin of the weak mass scaling in the global energy confinement time, in this section, we separately calculate the stored energy in the pedestal and core plasma regions. Then we compare the scaling of these two energies with the isotopic mass.

The edge pedestal energy is calculated using data from a high resolution ECE diagnostic [12] which measures the edge electron temperature profile. A typical example is shown in Fig. 6. The knee in the profile is identified manually. The density is determined from the interferometer vertical chord at 3.75m. The stored electron energy in the pedestal region which is shown schematically in Fig. 7 can then be calculated. We assume that the ion temperature at the pedestal is equal to the electron temperature so that the total pedestal energy can be calculated. The core energy is then calculated from the difference of the total thermal stored energy and the pedestal energy.

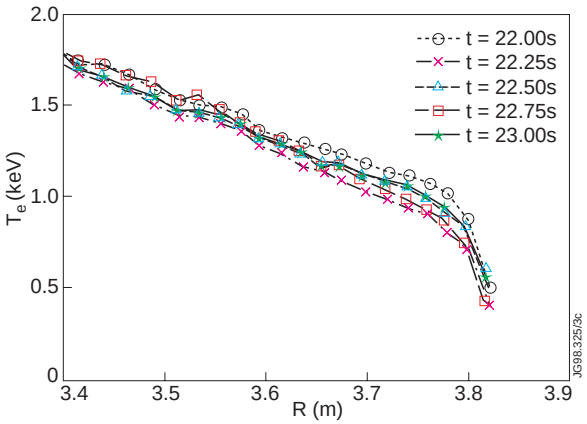

Fig. 6. Electron temperature profiles from the ECE diagnostic in the edge region for a series of time points during the steady state ELMy phase of a typical pulse.

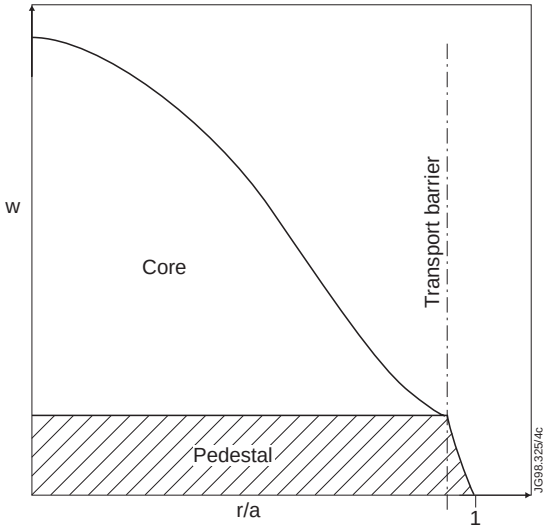

Fig. 7. A schematic representation of the stored energy density versus radius, the shaded region is the stored energy in the pedestal and the unshaded region is the stored energy in the core.

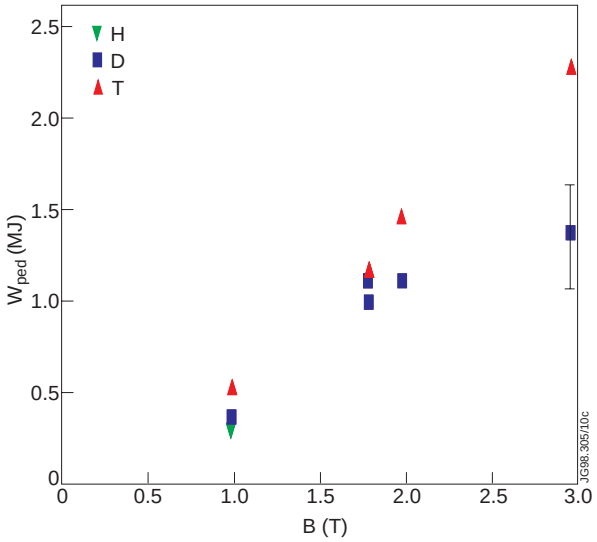

Fig. 8. Pedestal stored energy versus toroidal field B. The symbols are `t` H, `n` D, and `s` 10:90 D-T.

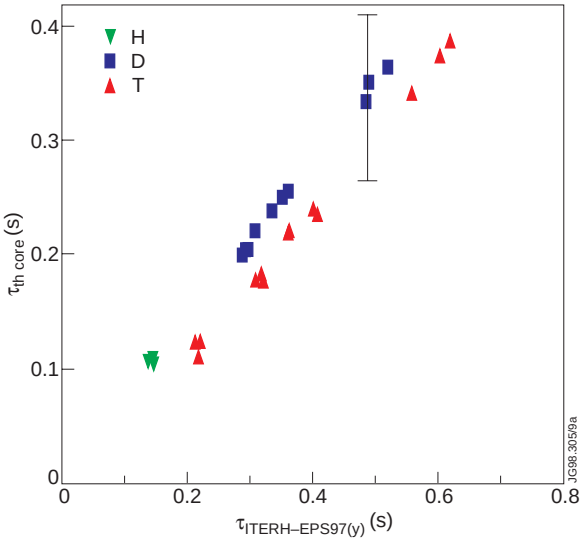

Fig. 9. Comparison of the thermal confinement in the plasma core versus the scaling expression of ITERH-EPS97(y).

First the scaling of the edge pedestal, in Fig. 8, the stored energy in the edge pedestal is shown versus the toroidal field for the matched power and density dataset of the previous section. The points to note are, first the strong dependence on toroidal field (or current), since the q is fixed in this dataset, and second the almost linear dependence on isotope mass. A simple fit to the data has the form

$$W_{ped} = 0.45\ B^{1.2}\ (M/2)^{0.96} \qquad (10)$$

A possible explanation for the strong mass dependence may be due to the diverse nature of the ELMs. For pulses in H, D and T with the same power input it is found that the fraction of

input power lost by the ELMs decreases when going from hydrogen to tritium, i.e. the power lost through the ELMs decreases with mass. A future paper [13] will discuss the effect of changing the isotope upon the ELMs in greater detail.

For the scaling of the core plasma we use the power and density matched dataset and compare $\tau_{thcore} = (W_{th} - W_{ped})/P_{loss}$ with the scaling expression for the ELMy H-mode Eq. (1) in Fig. 9. In this figure we can see that there is a clear offset in τ_{thcore} between the deuterium and tritium datasets. To eliminate the separation of the two data sets we find that we need to multiply equation (1) by $M^{-0.36}$ giving a mass dependence for the core of $\tau_{thcore} \propto M^{-0.16\pm0.1}$. This is close to the expected gyro-Bohm scaling for the core of $M^{-0.2}$. Thus to summarise the weak positive scaling of the total thermal stored energy mass is a combination of a negative index for the mass scaling of the core with a strong positive mass scaling of the edge.

V. LOCAL TRANSPORT ANALYSIS

A local transport analysis of almost the complete dataset was carried out using the TRANSP code. The main inputs to the code were the electron temperature and density profiles from the Lidar diagnostic [9] and the ion temperature and Zeff profiles from the charge exchange diagnostic [10].

The main analysis of the data set has been concentrated on the same small set of pulses having the same density and power input of Section II. In Fig. 10 the ion thermal diffusivity χ_i is shown versus radius for the pairs of deuterium and tritium pulses of Fig. 3. In the core confinement region the χ_i of the tritium pulse is larger than that of the deuterium pulse, however towards the edge region χ_i of the deuterium pulse exceeds that of the tritium.

The above analysis has been repeated for all of the shot pairs in the power matched data set. It is found that the pattern of Fig. 10 is repeated at other currents, i.e. the tritium χ_i being

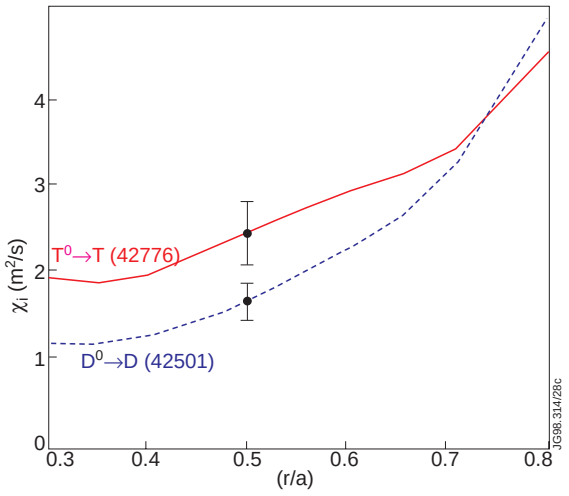

Fig. 10. Ion thermal conductivity versus normalised radius for the Deuterium and Tritium pulses of Fig. 3. The T pulse is 42776 and the D pulse is 42501.

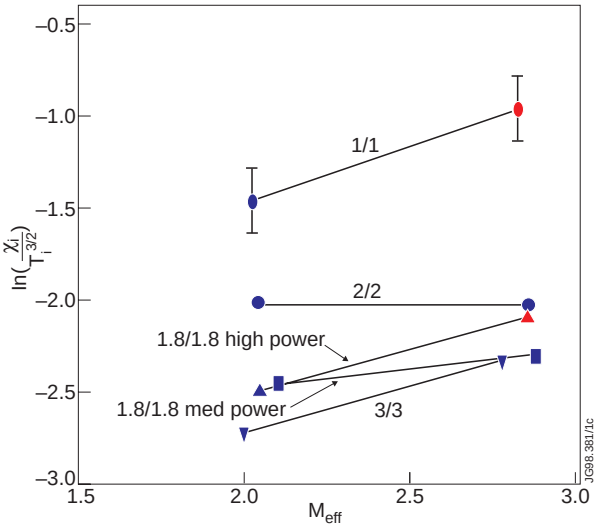

Fig. 11. Normalised ion thermal conductivity at r/a = 0.5 versus effective mass M for 5 pairs of pulses of the reduced dataset.

higher in the core region than the deuterium and the reverse occurring in the edge region. The χ_i at the r/a = 0.5 position is shown for the full dataset in Fig. 11. Here the χ_i has been normalised with respect to $T_i^{3/2}$ (at the r/a = 0.5 position). This particular normalisation presumes a gyro-Bohm type of scaling, however the scaling with mass is only slightly changed if a Bohm normalisation T_i is used. The reason for the normalisation is to account for the small differences in density between some of the pulses. Fig. 11 clearly shows that the χ_i increases with mass and the gyro-Bohm form $\chi_i \propto M^{1/2}$ Eq. (5) is consistent with the data. Fitting the complete dataset to a form $\chi_i \propto M^{\alpha} T_i^{3/2}/B^2$ gives $\alpha = 0.73 \pm 0.4$ slightly stronger than gyro-Bohm.

The scaling of both χ_e and χ_{eff} with M has also been investigated. Due to the small power flow through the electron channel the scatter in χ_e is found to be too large to obtain a scaling. The χ_{eff} was found to scale in a similar fashion to χ_I with a positive but somewhat weaker, mass dependence.

VI. SUMMARY

The dependence of the confinement of both ELM-free and ELMy H-modes on the hydrogenic isotopes H, D, D-T, T, has been analysed. The global confinement time in the ELM-free data has been found to decrease weakly with the isotope mass $\tau_{th} \propto M^{-0.25 \pm 0.22}$, whilst for the ELMy data the τ_{th} is essentially independent of mass. By separating the core and pedestal energies in the ELMy dataset we have shown that the core energy confinement decreases weakly with the isotope mass ($\tau_{th\ core} \propto M^{-0.16 \pm 0.1}$). In contrast the edge pedestal energy is found to increase almost linearly with mass M. The behaviour of the plasma core has been confirmed by a local transport analysis using the TRANSP code. The confinement in the core deteriorating with mass number in the form $\chi_i \propto M^{0.73 \pm 0.4}$.

The above scalings are in line with the theoretical expectation of the core region being dominated by gyro-Bohm transport and the edge dominated by the effect of the ELMs, an MHD phenomena.

ACKNOWLEDGEMENT

The authors would like to thank the whole of the JET Team, including all the technicians and the support staff, without whose dedication and hard work these experiments could not have taken place.

REFERENCES

[1] WAGNER, F., et al., in Controlled Fusion and Plasma Heating (Proc. 17th Eur. Conf. Amsterdam, 1990), Vol. 14B, Part I EPS Geneva (1990) 58.

[2] SCHISSEL, D.P. et al., Nucl. Fusion **29** (1989) 185. STALLARD, B.W. et al., Nucl. Fusion **30** (1990) 2235.

[3] KIKUCHI, M., et al., in Plasma Physics and Controlled Nuclear Fusion Research (Proc. 14th Int. Conf. Würzburg 1992) Vol. I. IAEA Vienna (1993) 189.

[4] TIBONE, F., et al., Nucl. Fusion **33** (1993) 1319.

[5] SCOTT, S.D., et al. in Fusion Energy (Proc. 16th Int. Conf. Montreal 1996) Vol. I, IAEA Vienna (1997) 573.

[6] GIBSON, A.G., APS presentation paper.

[7] ITER Confinement Database and Modelling Working Group, presented by J.G. Cordey, Energy Confinement Scaling and the Extrapolation to ITER plasma phys. Control. Fusion **39** (1997) B115-B127.

[8] H-MODE DATABASE WORKING GROUP, presented by D.P. SCHISSEL, Analysis of the ITER H-mode Confinement Database, in Controlled Fusion and Plasma Physics (Proc. 20th Eur. Conf., Lisbon, 1993) Vol. 17C, Part 1, European Physical Society, Geneva (1993) 103-106.

[9] GOWERS, C., BROWN, B.W., FAJEMIROKUN, H., NIELSEN, P., NIZIENKO, Y., SCHUNKE, B., Rev. Sci. Instrum. 66 (1), Jan '95 p. 471.

[10] VON HELLERMANN, M., SUMMERS, H.P., Atomic and Plasma Material Interaction Processes in Controlled Thermonuclear Fusion, editor R. Janev, 'Elsevier Science Publishers 1993', 135-164, JET-P(93)34.

[11] THOMAS, P.R., et al. Phys. Rev. Lett. 80 (1998) 5548.

[12] BARTLETT, D.V. et al., Proc. 9th Int. Workshop on ECE and ERCRH, Borrego Springs, U.S.A. (1995).

[13] BHATNAGAR, V., et al., To be submitted to Nucl. Fusion.